

may have accentuated this effect. The activation of dendritic Na⁺ channels does not necessarily lead to fully overshooting action potentials but may simply elevate EPSP amplitude. The slow kinetics of LVA Ca²⁺ currents, and possibly persistent Na⁺ currents, could also extend EPSP duration, prolonging the time available for synaptic integration (2, 15). Dendritic Na⁺ and Ca²⁺ channels are therefore capable of enhancing the efficacy of more distal and widely distributed synaptic contacts by increasing both the strength and duration of synaptic input over that predicted by the passive cable properties of the neuron.

Activation of voltage-gated Na⁺ and Ca²⁺ channels in dendrites may also provide an important local signal for dendritic integration of synaptic inputs. Subthreshold synaptic activation of dendritic voltage-gated channels could have very localized effects on the membrane time constant, local ionic driving forces, ligand-gated channel conductances, and the influx of Ca²⁺. Such local events, perhaps confined to the specific dendritic branch where synaptic input occurs, could affect the spatial and temporal summation of synaptic inputs occurring in that region and would provide a limited space in which Ca²⁺-dependent intracellular events can take place (16). Subthreshold synaptic activation of dendritic channels may provide mechanisms for highly localized, short- or long-duration modifications in the process of synaptic integration.

In contrast, our results demonstrate directly that Ca²⁺ channels are opened by action potentials backpropagating into the dendrites, as has been suggested with fluorescence imaging (6). We demonstrate that rises in intracellular Ca²⁺ are due, at least in part, to the opening of HVA Ca²⁺ channels. The opening of these channels can occur tens of milliseconds after the action potential (Fig. 4B) and may be related to the repolarization openings described for HVA Ca²⁺ channels (17). Activation of the larger conductance HVA Ca²⁺ channels will provide an influx of Ca²⁺ throughout an extended portion of the dendritic arborization (defined by the extent of action potential propagation). The spatial domain of the effects of these channels will therefore be much more extensive compared with their effects after subthreshold activation. Thus, the voltage-gated channels in CA1 apical dendrites may modify synaptic strength over either localized or broad areas of the dendrites (18).

REFERENCES AND NOTES

1. P. Andersen, M. Raastad, J. F. Storm, *Cold Spring Harbor Symp. Quant. Biol.* **55**, 81 (1990); K. M. Harris, F. E. Jensen, B. Tsao, *J. Neurosci.* **12**, 2685 (1992).
2. S. W. Jaslove, *Neuroscience* **47**, 495 (1992); N.

- Spruston, D. Jaffe, S. H. Williams, D. Johnston, *J. Neurophysiol.* **70**, 781 (1993); N. Spruston, D. Jaffe, D. Johnston, *Trends Neurosci.* **17**, 161 (1994).
3. R. E. Westenbroek, M. K. Ahljian, W. A. Catterall, *Nature* **347**, 281 (1990); R. Llinas, M. Sugimori, D. E. Hillman, B. Cherksey, *Trends Neurosci.* **15**, 351 (1992); R. E. Westenbroek et al., *Neuron* **9**, 1099 (1992).
4. H. Markram and B. Sakmann, *Proc. Natl. Acad. Sci. U.S.A.* **91**, 5207 (1994).
5. M. M. Usovich, M. Sugimori, R. Llinas, *Neuron* **9**, 1185 (1992); G. J. Stuart and B. Sakmann, *Nature* **367**, 69 (1994).
6. H. Miyakawa et al., *Neuron* **9**, 1163 (1992); B. R. Christie, L. S. Elliot, H. Miyakawa, K. Ito, D. Johnston, *J. Neurophysiol.*, in press; D. Jaffe et al., *Nature* **357**, 244 (1992).
7. J. C. Magee and D. Johnston, *J. Physiol. (London)*, in press.
8. P. Sah, A. J. Gibb, P. W. Gage, *J. Gen. Physiol.* **91**, 373 (1988); N. Ogata and H. Tatebayashi, *Pflügers Arch.* **416**, 594 (1990).
9. R. E. Fisher, R. Gray, D. Johnston, *J. Neurophysiol.* **64**, 91 (1990); D. J. Mogul and A. P. Fox, *J. Physiol. (London)* **433**, 259 (1991); T. J. O'Dell and B. E. Alger, *ibid.* **436**, 739 (1991).
10. Hippocampal slices (400 μm) were prepared from 5- to 8-week-old Sprague-Dawley rats according to standard procedures, and individual neurons were viewed as described [G. J. Stuart, H. U. Dodt, B. Sakmann *Pflügers Arch.* **423**, 511 (1993)]. The external solution contained 124 mM NaCl, 2.5 mM KCl, 1.2 mM NaPO₄, 26 mM NaHCO₃, 2.0 mM CaCl₂, 1.0 mM MgCl₂, and 20 mM dextrose and was bubbled with 95% O₂, 5% CO₂ at ~22°C.
11. Somatic voltage was recorded with an Axoclamp 2A amplifier (Axon Instruments) in "bridge" mode. Whole-cell recording pipettes (2 to 4 megohms) were filled with 140 mM KMeSO₄, 10 mM Hepes, 0.5 mM EGTA, 3.0 mM MgCl₂, 4.0 mM sodium adenosine triphosphate, and 0.1 mM tris-guanosine triphosphate (pH 7.4 with KOH). For Na⁺ channel

- recordings, pipettes (6 to 10 megohms) contained 110 mM NaCl, 30 mM tetraethylammonium chloride (TEACl), 10 mM Hepes, 2.0 mM CaCl₂, and 5 mM 4-aminopyridine (pH 7.4 with TEOH). Na⁺ channel records were analog filtered at 2 kHz (-3 db; 8-pole Bessel) and digitized at 20 kHz. For Ca²⁺ channel recordings, the pipette solution contained 20 mM BaCl₂, 110 mM TEACl, 10 mM Hepes, 5 mM 4-aminopyridine, and 1 μM TTX (pH 7.4 with TEOH). Ca²⁺ channel records were analog filtered at 2 or 1 kHz and digitized at 10 kHz. For single-electrode recordings, V_m (-60 to -70 mV) was determined by later rupture of the patch to whole-cell recording mode. For focal extracellular stimulation, a glass pipette (tip diameter 10 μm) or a single-etched platinum wire (tip diameter <5 μm) was placed near the dendrite under study.
12. P. T. Ellinor et al., *Nature* **32**, 455 (1993); J. F. Zhang et al., *Neuropharmacology* **363**, 1075 (1993); T. Schneider et al., *Biophys. J.* **66**, A423 (1994).
13. E. M. Fenwick, A. Marty, E. Neher, *J. Physiol. (London)* **331**, 599 (1982); C. Alzheimer, P. C. Schwindt, W. E. Crill, *J. Neurosci.* **13**, 660 (1993).
14. B. Hille, *Ionic Channels of Excitable Membranes* (Sinauer, Sunderland, MA, 1992).
15. R. D. Traub and R. Llinas, *J. Neurophysiol.* **42**, 476 (1979); R. A. Deisz, G. Fortin, W. Zieglgansberger, *ibid.* **65**, 371 (1991).
16. G. White, W. B. Levy, O. Steward, *ibid.* **64**, 1186 (1990); D. B. Jaffe et al., *ibid.* **71**, 1065 (1993).
17. R. E. Fisher, R. Gray, D. Johnston, *ibid.* **64**, 91 (1990); O. Thibault, N. M. Porter, P. W. Landfeld, *Proc. Natl. Acad. Sci. U.S.A.* **90**, 11792 (1993).
18. D. Johnston, W. Williams, D. Jaffe, R. Gray, *Annu. Rev. Physiol.* **54**, 489 (1992); D. M. Kullmann, D. J. Perkel, T. Manabe, R. Nicoll, *Neuron* **9**, 1175 (1992).
19. We thank C. Colbert for comments on the manuscript. Supported by NIH grants NS09482, NS11535, MH44754, and MH48432.

5 December 1994; accepted 16 February 1995

Silver as a Probe of Pore-Forming Residues in a Potassium Channel

Qiang Lü and Christopher Miller*

In voltage-dependent potassium channels, the molecular determinants of ion selectivity are found in the P (pore) region, a stretch of 21 contiguous residues. Cysteine was introduced at each P region position in a Shaker potassium channel. Residues projecting side chains into the pore were identified by means of channel inhibition by a sulfhydryl-reactive potassium ion analog, silver ion. The pattern of silver ion reactivity contradicts a β barrel architecture of potassium channel pores.

Voltage-gated ion channels of excitable cell membranes operate as expert inorganic chemists. K⁺ channels, for instance, discriminate well among the alkali metal cations; in some cases they transport K⁺ 1000 times more efficiently than Na⁺ (1). Because ions traverse channel proteins by diffusion through narrow, water-filled pores, questions of ion selectivity have focused on the nature of the chemical groups that line these pores. In voltage-gated K⁺ channels, the selectivity-determining groups reside in

the P region, a conserved hairpin sequence that enters and leaves the membrane from the extracellular side (2-4). Other transmembrane sequences contribute to the cytoplasmic end of K⁺ channel pores (5), but residues that strongly affect ion selectivity have been found only in the P region. K⁺ channels are tetrameric, with P regions of the four subunits symmetrically surrounding the conduction pathway (6-8), but the chemistry of K⁺ ligation within the pore is unknown (9). To ascertain which residues project side chains into the pore lumen, we used cysteine susceptibility analysis (10), in which individual residues in the pore-forming sequence are mutated to cysteine and the sensitivity of the resulting channels to

Howard Hughes Medical Institute and Graduate Department of Biochemistry, Brandeis University, Waltham, MA 02254, USA.

*To whom correspondence should be addressed.

aqueous thiol-labeling reagents is assessed.

We modified this approach in response to two problems that impeded its use with K^+ channels. The first problem is that organic thiol-directed reagents are too large to reach the narrow ($\sim 3 \text{ \AA}$) confines of the pore. Because these channels efficiently exclude solutes other than K^+ and its analogs, the ideal cysteine-reactive probe for our purposes would be a small, inorganic, monovalent cation. Ag^+ serves well as such a reagent. The radius of the Ag^+ cation, 1.26 \AA , is within 0.07 \AA of that of K^+ (11); moreover, Ag^+ , like K^+ , allows rapid exchange of inner-shell water molecules in aqueous solution (12) and readily permeates the gramicidin A channel (13). Chemically, Ag^+ is a soft Lewis acid that reacts avidly with the thiolate group to form a strong covalent S-Ag bond (14).

The second problem is the P region's notorious sensitivity to point mutation (4, 15): For most positions, substitution of cysteine alters or eliminates channel function. Because K^+ channels are tetrameric, such mutations introduce four cysteine residues into the assembled complex. Accordingly, we engineered channels to contain only a single cysteine substitution by coexpressing a small fraction of cysteine-mutant subunits with a preponderance of wild-type P region Shaker channel. The cysteine-substituted subunit carried a "ball-and-chain" N-type inactivation domain (16), which was deleted in the subunits lacking the cysteine mutation. Thus, in a voltage-clamp experiment (Fig. 1), the inactivating component of the current is solely the result of channels with "ball-tagged" subunits bearing a cysteine mutation (6, 8).

Potassium channels were robustly expressed in *Xenopus laevis* oocytes injected with mixtures of complementary RNAs that coded for wild-type, inactivation-re-

moved (Shaker-IR) subunits and ball-tagged cysteine mutants (17). The inactivating component of the current represents channels carrying at least one cysteine-labeled subunit, whereas the steady-state current reflects wild-type Shaker-IR channels (Fig. 1). Most of the inactivating current

arises from channels with only a single cysteine residue; there was a 3.3-fold difference between the inactivation time constant (8 ms) and that in channels with four inactivation domains (8). The inactivating component showed conventional voltage dependence of activation; hence we are con-

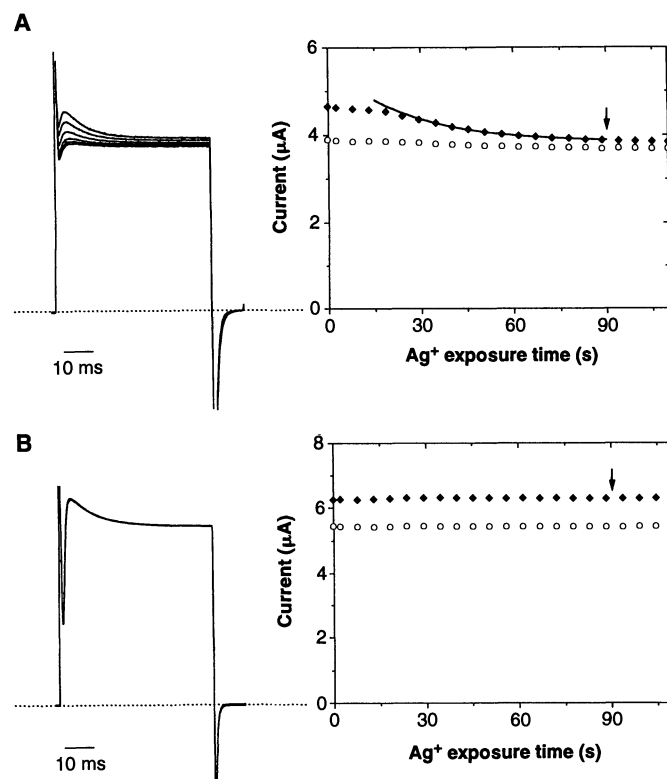


Fig. 2. Inhibition by Ag^+ : susceptible and unresponsive substitutions. Cysteine-labeled channels were expressed as in Fig. 1, and 50-ms pulses (-90 to 40 mV) were given at 3-s intervals (every second pulse displayed). After the first pulse, bath solution containing 200 nM Ag^+ was applied, and each response was recorded for the next 2 to 3 min. Right panel: time course of peak (\blacklozenge) and steady-state (\circ) current after application of Ag^+ . Ag^+ was removed from bath solutions where indicated by arrow. (A) A responsive residue, V8. The solid curve shows a single-exponential fit to the inhibition time course. (B) An unresponsive residue, A6.

Table 1. Susceptibility of cysteine-substituted channels by extracellular Ag^+ . Shaker channels containing cysteine substituted at each P region position were exposed to 200 nM Ag^+ for 90 s. The relative K^+ current remaining after Ag^+ exposure is reported for the inactivating (f_{cys}) and steady-state (f_{wt}) components. The apparent second-order rate constants, k_{app} , for the Ag^+ -susceptible residues were estimated from the time constants of inhibition, the total Ag^+ concentration, and the negative logarithm of the acid constant (pK_a) of 8.6 for the cysteine thiol. Data represent mean \pm SE of three to five measurements, each in a separate oocyte. Missing values of k_{app} indicate no inhibition and thus no time constant of inhibition.

Position	f_{cys}	f_{wt}	k_{app} ($10^6 \text{ M}^{-1} \text{ s}^{-1}$)	Deduced exposure
Wild-type	—	0.99 ± 0.01	—	—
P0	0.64 ± 0.06	1.05 ± 0.04	7.8 ± 0.8	Exposed
D1	>0.9	0.92 ± 0.05	—	Exposed (25, 26)
A2	<0.84	0.97 ± 0.03	<0.4	Rarely exposed?
F3	>0.9	0.95 ± 0.05	—	Buried
W4	0.66 ± 0.04	1.02 ± 0.01	5.6 ± 0.3	Exposed
W5	0.46 ± 0.1	0.89 ± 0.06	5.9 ± 0.5	Exposed
A6	>0.95	1.03 ± 0.02	—	Buried
V7	>0.95	1.04 ± 0.03	—	Buried
V8	0.36 ± 0.06	0.91 ± 0.03	7 ± 1	Exposed
T9	>0.95	1.05 ± 0.01	—	Undetermined
M10	>0.95	1.04 ± 0.05	—	Undetermined
T11	>0.95	1.07 ± 0.01	—	Undetermined
T12	>0.95	1.09 ± 0.01	—	Undetermined
V13	0.54 ± 0.06	0.94 ± 0.02	2 ± 0.2	Exposed
Y15	0.07 ± 0.02	1.00 ± 0.02	13.0 ± 1.7	Exposed
G16	>0.95	1.04 ± 0.03	—	Buried
D17	0.70 ± 0.05	0.94 ± 0.05	5.4 ± 0.9	Exposed
M18	0.37 ± 0.08	0.93 ± 0.01	6.5 ± 0.5	Exposed
T19	0.14 ± 0.02	0.95 ± 0.02	4.5 ± 0.8	Exposed
P20	0.33 ± 0.06	0.93 ± 0.02	10 ± 1	Exposed

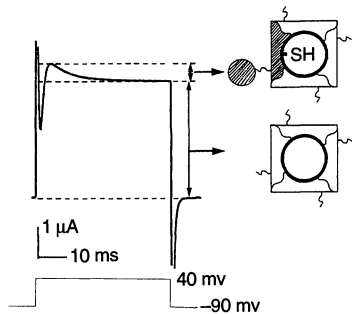


Fig. 1. Voltage activation response of channels formed from a 4:1 mixture of Shaker-IR subunits and ball-tagged Shaker subunits with cysteine substituted at a known pore determinant, W434, which is position W4 in our numbering system (18). Icons represent Shaker channels composed of IR subunits with a wild-type P region (unshaded) and cysteine-substituted subunits with N-type inactivation intact (shaded). SH, sulfhydryl group.

vident that the cysteine substitution does not disrupt the overall channel structure.

Shaker channels carrying cysteine at the selectivity-determining residue V8 (18) became sensitive to Ag^+ (Fig. 2A). The inactivating current was inhibited by submicromolar amounts of Ag^+ on a time scale of 1 min, whereas the Shaker-IR background remained unchanged. This inhibition was irreversible after washout of Ag^+ and required cysteine in the inactivating subunit. We therefore conclude that the cysteine side chain is exposed to the pore lumen at position V8. Moreover, because these experiments used short pulses and long hyperpolarized interpulse intervals, residue V8 was accessible from the external solution in the channel's closed state; longer pulse durations did not enhance the rate of Ag^+ inhibition. Certain residues that were substituted with cysteine, such as A6 (Fig. 2B), were unresponsive to Ag^+ . With cysteine substituted at this position, the inactivating and steady-state components of the current each changed less than 5% after exposure to Ag^+ .

We introduced cysteine in this way at all 21 P region positions. All mutants produced

inactivating voltage-dependent K^+ currents except for G14, a critical structural determinant of the pore (4, 19). Of the 20 functional substitutions (Table 1), 10 were irreversibly inhibited by external Ag^+ (20 to 200 nM) in 1 to 5 min. At several residues (Y15 and T19), inhibition was nearly complete, but at most positions it remained partial even after long exposure to Ag^+ ; this observation suggests that formation of the Ag adduct modifies but does not destroy channel activity. Representative records that span the range of Ag^+ responses are shown in Fig. 3.

Two of the Ag^+ -sensitive positions were previously known to be accessible to reversible pore-blockers from the external aqueous phase. The residue at V8 affects the channel's selectivity among close K^+ analogs; when histidine is placed here, the Kv2.1 channel becomes sensitive to external Zn^{2+} (20). Likewise, in Shaker channels, substitutions at T19 interact directly with external tetraethylammonium (TEA) (21), Cd^{2+} (22), or Cu^{2+} . Detailed examination of TEA inhibition (7) localizes this position at the extreme external opening of

the pore, where it widens to a diameter of $\sim 8 \text{ \AA}$.

Six of the Ag^+ -susceptible residues (W4, W5, V8, V13, Y15, and D17) are involved in K^+ permeation (4, 15, 19, 20, 23). The mechanism by which Ag^+ alters channel function at these positions is unknown; our experiments sought only to establish which residues are Ag^+ -sensitive. These residues were all inhibited with similar second-order rate constants in the range of $10^7 \text{ M}^{-1} \text{ s}^{-1}$, similar to that of K^+ permeation itself; hence, the Ag^+ -thiolate reaction cannot be viewed as reflecting a rarely exposed configuration of the cysteine side chain. However, one residue (A2) was inhibited by Ag^+ at a much lower rate than that seen in other susceptible residues.

The residues at the nine remaining positions were unaffected by Ag^+ on our experimental time scale. These unresponsive residues are subject to several competing interpretations. One possibility is that the residues react with Ag^+ but are located too far away from the pore axis to influence K^+ permeation. This explanation is plausible for residues more distant than the width of two or three water molecules, because the difference between S-H and S-Ag groups should be sensed only at close range; in effect, the "mutation" produced by reaction of a thiol group with Ag^+ is subtle from the perspective of a K^+ ion in the pore. This effect is almost certainly the reason that residue D1 is unresponsive to Ag^+ ; this residue, which is 10 to 15 \AA away from the pore axis (6, 24, 26), contributes a carboxylate group to the charybdotoxin receptor in the external vestibule. On the other hand, the Ag^+ insensitivity of residues A6, V7, and G16 cannot be explained by remoteness from the pore because these residues are sandwiched in linear sequence between Ag^+ -sensitive positions known to influence K^+ permeation. The most straightforward explanation is that these side chains project into the bulk of the protein, away from the pore lumen. This is probably also the case for residue F3, which lies between the sensitive residues A2 and W4.

The four contiguous residues T9, M10, T11, and T12 are all unresponsive to Ag^+ . One of these, T11, specifically influences inhibition by internally applied TEA (3). It is natural to suggest, then, that external Ag^+ may fail to gain access to some of these residues because they lie on the cytoplasmic side of a "gate" that occludes the pore in the closed state. Tests of this unsupported idea will require internal application of Ag^+ to Shaker channels from which the seven natural cysteines have been removed (27), because internal Ag^+ powerfully inhibits wild-type Shaker.

A visual summary (Fig. 4) places our results in the context of previously localized

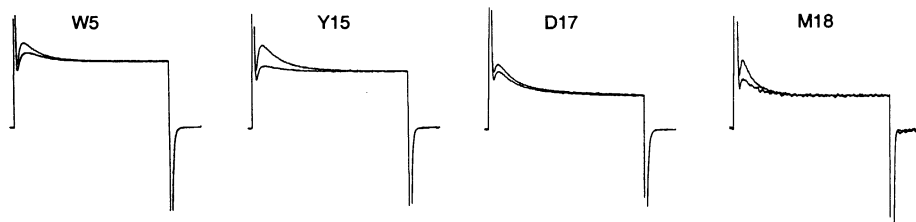
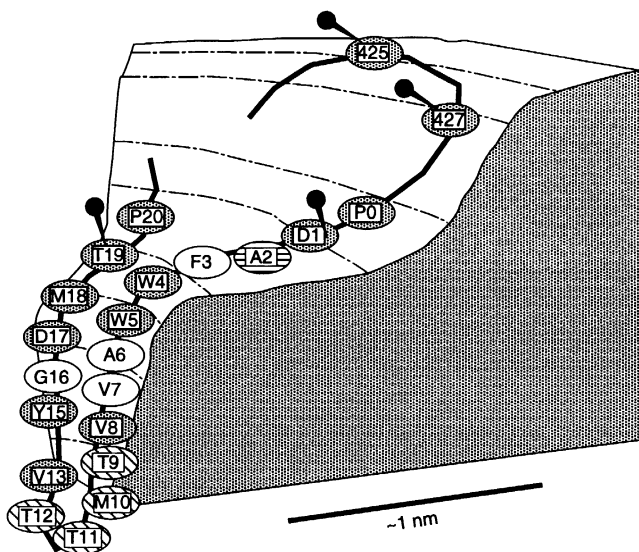


Fig. 3. Silver inhibition at several susceptible positions. Channels substituted with cysteine at the indicated positions were exposed to 200 nM Ag^+ as shown in Fig. 2. Each panel shows the response to a 50-ms pulse just before Ag^+ and after 1.5 min of Ag^+ exposure. Maximum currents ranged from 0.8 to 8 μA .

Fig. 4. Topography of the external pore and vestibule of the Shaker K^+ channel. A hypothetical single Shaker subunit, a 90° sector of the outer pore region and vestibule, is displayed. Residues studied here are indicated by P-region numbering (18); residues F425 and K427 are also indicated by Shaker numbering. Push pins indicate residues whose positions relative to the pore axis were previously established by mapping with reversible pore-blockers. Shaded residues have side chains that are proposed to project into the aqueous pore or vestibule. Unshaded residues are Ag^+ -unresponsive positions that are proposed to project away from the aqueous phase. Diagonal stripes indicate residues whose insensitivity to Ag^+ cannot be clearly interpreted in terms of side chain projection. The reactivity of residue A2 (horizontal stripes) is slower than that of the other Ag^+ -responsive residues.



residues. This structural model, experimentally based on side chain interactions alone, places residues in three-dimensional space on a single subunit (hence a 90° sector) of the homotetrameric K⁺ channel and shows the extent of side chain exposure to the pore lumen or external vestibule. As a structural hypothesis, the model is necessarily crude, but its consistency with the localization of residues gathered by independent methods is encouraging (7, 21, 25, 26). Although the model eschews explicit suggestions about backbone secondary conformation, the exposure pattern of the NH₂-terminal side of the P region (residues P0 to T9) is consistent with α -helical periodicity, as has been suggested in some models of the K⁺ channel pore (28); the exposure pattern is inconsistent with a pore formed as an eight-stranded β barrel, as envisioned in other models (3, 29).

With respect to ion selectivity mechanisms, these results allow us to draw two specific conclusions about a subset of P region residues. First, the residues projecting inward to line the narrow part of the pore begin beyond residue F3, at W4 or W5, not at P0. Second, it is now clear that among the P region's four aromatic side chains, three point toward the pore lumen: W4, W5, and Y15. Thus, the proposal (7, 30) that K⁺ in the pore is coordinated in a cage of π electrons, though in contention (4, 9), remains viable.

REFERENCES AND NOTES

- G. Yellen, *J. Gen. Physiol.* **84**, 157 (1984); J. Neyton and C. Miller, *ibid.* **92**, 569 (1988).
- H. A. Hartmann *et al.*, *Science* **251**, 942 (1991).
- G. Yellen, M. E. Jurman, T. Abramson, R. MacKinnon, *ibid.*, p. 939.
- L. Heginbotham, Z. Lu, T. Abramson, R. MacKinnon, *Biophys. J.* **66**, 1061 (1994).
- K. L. Choi, C. Mossman, J. Aube, G. Yellen, *Neuron* **10**, 533 (1993); P. A. Slesinger, Y. N. Jan, L. Y. Jan, *ibid.* **11**, 739 (1993); G. A. Lopez, Y. N. Jan, L. Y. Jan, *Nature* **367**, 179 (1994).
- R. MacKinnon, *Nature* **350**, 232 (1991).
- L. Heginbotham and R. MacKinnon, *Neuron* **8**, 483 (1992).
- R. MacKinnon, R. W. Aldrich, A. W. Lee, *Science* **262**, 757 (1993).
- C. Miller, *ibid.* **261**, 1692 (1993).
- M. H. Akabas, D. A. Stauffer, M. Xu, A. Karlin, *ibid.* **258**, 307 (1992); M. H. Akabas, C. Kaufmann, T. A. Cook, P. Archdeacon, *J. Biol. Chem.* **269**, 14865 (1994); M. Xu and M. H. Akabas, *ibid.* **268**, 21505 (1993); M. H. Akabas, C. Kaufmann, P. Archdeacon, A. Karlin, *Neuron* **13**, 919 (1994); R. D. Zuhlke *et al.*, *Soc. Neurosci. Abstr.* **20**, 864 (1994).
- R. S. Nyholm, *Proc. Chem. Soc.* **1961**, 273 (1961).
- G. W. Liesegang, M. M. Farrow, F. A. Vazquez, N. Purdie, E. M. Eyring, *J. Am. Chem. Soc.* **99**, 3240 (1977).
- O. S. Andersen, personal communication.
- I. G. Dance, *Polyhedron* **5**, 1037 (1986).
- L. Heginbotham, thesis, Harvard University (1993).
- T. Hoshi, W. N. Zagotta, R. W. Aldrich, *Science* **250**, 533 (1990).
- Potassium channels were expressed in *Xenopus* oocytes with *Shaker* H4 cDNA or *Shaker*-IR channels lacking residues 6 to 46 (25). Two independent clones of each mutation were characterized. RNA (0.2 to 0.5 ng) containing wild-type and cysteine-substituted P region was injected at an approximate ratio of 4:1. Injected oocytes were kept 2 to 3 days at 18°C until recording by two-electrode voltage clamp (Warner Instruments, OC-725B). The bath solution contained 96 mM NaNO₃, 2 mM KNO₃, 0.3 mM Ca(NO₃)₂, 1 mM Mg(NO₃)₂, and 10 mM Hepes-NaOH (pH 7.1). AgNO₃ stock solutions were stored in the dark before dilution in the experimental solution. Ag-AgCl electrodes were connected to the bath by means of fresh salt bridges containing 300 mM NaNO₃. Recording microelectrodes (0.2 to 0.8 megohms) were filled with 3 M KCl. Voltage commands and current acquisition were controlled with a Microstar DAP3200e acquisition board. Perfusion was controlled manually (exchange time ~10 s).
- For brevity, we number the P region from P0 to P20, beginning with *Shaker* residue P430 and ending with P450. Abbreviations for the amino acid residues are as follows: A, Ala; D, Asp; F, Phe; G, Gly; K, Lys; M, Met; P, Pro; T, Thr; V, Val; W, Trp; and Y, Tyr.
- L. Heginbotham, T. Abramson, R. MacKinnon, *Science* **258**, 1152 (1992).
- M. de Biasi, J. A. Drewe, G. E. Kirsch, A. M. Brown, *Biophys. J.* **65**, 1235 (1993).
- R. MacKinnon and G. Yellen, *Science* **250**, 276 (1990).
- G. Yellen, D. Sodickson, T.-Y. Chen, M. E. Jurman, *Biophys. J.* **66**, 1068 (1994).
- G. E. Kirsch *et al.*, *Neuron* **8**, 499 (1992); M. Tagliatela *et al.*, *Pfluegers Arch.* **423**, 104 (1993); E. Perozo, R. MacKinnon, F. Bezanilla, E. Stefani, *Neuron* **11**, 353 (1993).
- R. MacKinnon, L. Heginbotham, T. Abramson, *Neuron* **5**, 767 (1990).
- S. A. N. Goldstein, D. J. Pheasant, C. Miller, *ibid.* **12**, 1377 (1994).
- P. Hidalgo and R. MacKinnon, *Science* **268**, 307 (1995).
- L. M. Boland, M. E. Jurman, G. Yellen, *Biophys. J.* **66**, 694 (1994).
- S. R. Durell and H. R. Guy, *ibid.* **62**, 238 (1992).
- C. Miller, *Science* **252**, 1092 (1991); S. Bogusz, A. Boxer, D. D. Busath, *Protein Eng.* **5**, 295 (1992).
- R. A. Kumpf and D. A. Dougherty, *Science* **261**, 1708 (1993).
- We thank D. Naranjo for advice throughout these experiments and L. Heginbotham for critical reading of the manuscript. Supported in part by NIH grant GM-31768.

20 October 1994; accepted 29 December 1994

Revealing the Architecture of a K⁺ Channel Pore Through Mutant Cycles with a Peptide Inhibitor

Patricia Hidalgo and Roderick MacKinnon

Thermodynamic mutant cycles provide a formalism for studying energetic coupling between amino acids on the interaction surface in a protein-protein complex. This approach was applied to the *Shaker* potassium channel and to a high-affinity peptide inhibitor (scorpion toxin) that binds to its pore entryway. The assignment of pairwise interactions defined the spatial arrangement of channel amino acids with respect to the known inhibitor structure. A strong constraint was placed on the *Shaker* channel pore-forming region by requiring its amino-terminal border to be 12 to 15 angstroms from the central axis. This method is directly applicable to sodium, calcium, and other ion channels where inhibitor or modulatory proteins bind with high affinity.

A remarkable property of K⁺ channels is their ability to discriminate nearly perfectly between K⁺ and Na⁺ ions. Recent studies have identified several regions of K⁺ channel proteins that mediate ion conduction (1, 2). However, all evidence indicates that a short stretch of amino acids, the P (pore) region, is the sole determinant of K⁺ selectivity (3). Scorpion toxins interact intimately with this region and can be used as a structural template to deduce the spatial organization of P region residues (4).

To assign the location of channel residues (Fig. 1A) with respect to the toxin structure (Fig. 1B), we applied a systematic analysis based on the following intuitive principle. If amino acid *a* on the toxin interacts with amino acid *b* on the channel, then the effect (on the toxin-channel equilibrium) of mutating residue *a* should depend on whether *b* is mutated. The cross influence of one mutation on the effect of another can be quantified using a thermo-

dynamic cycle (Fig. 1C) to analyze experiments where *a* and *b* are mutated separately and then together. The arrows connecting each toxin-channel pair refer to mutation of either the toxin (horizontal arrows) or the channel (vertical arrows). Each arrow number represents the factor by which affinity changes along the direction of the arrow—that is, the equilibrium inhibition constant (K_i) of the toxin-channel pair at the tail of the arrow divided by the K_i value of the toxin-channel pair at the arrowhead. For example, $X1$ equals $K_i(\text{wt:wt})/K_i(\text{mut:wt})$, where wt:wt is the wild-type toxin-wild-type channel pair and mut:wt is the mutant toxin-wild-type channel pair (5). The affinity change in going from the wild-type toxin-wild-type channel interaction (Fig. 1C, upper left) to the mutant toxin-mutant channel interaction (Fig. 1C, lower right) must be the same regardless of the pathway taken; therefore, we have

$$X1 \cdot Y1 = X2 \cdot Y2 \quad (1)$$

Dividing both sides of Eq. 1 by $X2 \cdot Y1$ leads

Department of Neurobiology, Harvard Medical School, Boston, MA 02115, USA.